RL-TR-94-97
Final Technical Report
July 1994

EVALUATION OF CURRENT BIASED INTEGRATED OPTICAL PROCESSORS BASED ON BISTABLE DIODE ELEMENTS

Cornell University

C.L. Tang and P.D. Swanson (Cornell University)
M.A. Parker and S.I. Libby (Rome Laboratory)

DTIC
ELECTE
OCT 1 4 1994
S D
G

AD-A285 532

APPROVED FOR PUBLIC RELEASE; DISTRIBUTION UNLIMITED.

DTIC QUALITY INSPECTED 2

9 4 1 0 8

94-32185

Rome Laboratory
Air Force Materiel Command
Griffiss Air Force Base, New York

This report has been reviewed by the Rome Laboratory Public Affairs Office (PA) and is releasable to the National Technical Information Service (NTIS). At NTIS it will be releasable to the general public, including foreign nations.

RL-TR-94-97 has been reviewed and is approved for publication.

APPROVED: Michael A Parker

MICHAEL A. PARKER
Project Engineer

FOR THE COMMANDER: Luke L Lucas

LUKE L. LUCAS, Colonel, USAF
Deputy Director
Surveillance & Photonics Directorate

If your address has changed or if you wish to be removed from the Rome Laboratory mailing list, or if the addressee is no longer employed by your organization, please notify RL (OCPB) Griffiss AFB NY 13441. This will assist us in maintaining a current mailing list.

Do not return copies of this report unless contractual obligations or notices on a specific document require that it be returned.

REPORT DOCUMENTATION PAGE

Form Approved
OMB No. 0704-0188

Public reporting burden for this collection of information is estimated to average 1 hour per response, including the time for reviewing instructions, searching existing data sources, gathering and maintaining the data needed, and completing and reviewing the collection of information. Send comments regarding this burden estimate or any other aspect of this collection of information, including suggestions for reducing this burden, to Washington Headquarters Services, Directorate for Information Operations and Reports, 1215 Jefferson Davis Highway, Suite 1204, Arlington, VA 22202-4302, and to the Office of Management and Budget, Paperwork Reduction Project (0704-0188), Washington, DC 20503

1. AGENCY USE ONLY (Leave Blank)	2. REPORT DATE	3. REPORT TYPE AND DATES COVERED
	July 1994	Final Mar 93 - Jul 93

4. TITLE AND SUBTITLE
EVALUATION OF CURRENT BIASED INTEGRATED OPTICAL PROCESSORS BASED ON BISTABLE DIODE ELEMENTS

5. FUNDING NUMBERS
C - F30602-93-C-0068
PE - 62702F
PR - 4600
TA - P3
WU - PK

6. AUTHOR(S)
C.L. Tang and P.D. Swanson (Cornell University)
M.A. Parker and S.I. Libby (Rome Laboratory)

7. PERFORMING ORGANIZATION NAME(S) AND ADDRESS(ES)
Cornell University
120 Day Hall
Ithaca NY 14853-2801

8. PERFORMING ORGANIZATION REPORT NUMBER
N/A

9. SPONSORING/MONITORING AGENCY NAME(S) AND ADDRESS(ES)
Rome Laboratory (OCPB)
25 Electronic Pky
Griffiss AFB NY 13441-4515

10. SPONSORING/MONITORING AGENCY REPORT NUMBER
RL-TR-94-97

11. SUPPLEMENTARY NOTES
Rome Laboratory Project Engineer: Michael A. Parker/OCPB/(315) 330-7671

12a. DISTRIBUTION/AVAILABILITY STATEMENT
Approved for public release; distribution unlimited.

12b. DISTRIBUTION CODE

13. ABSTRACT (Maximum 200 words)
Three optical switching elements have been designed, fabricated and tested for use in an integrated, optical signal processor. The first, and optical NOR logic gate, uses gain quenching as a means of allowing one (or more) light beam(s) to control the output light. This technique, along with the use of a two-pad bistable output laser, is uded in the demonstration of the feasibility of the second device, an all optical RS flip-flop. The third device consists of a broad area orthogonal mode switch laser, whose corollary outputs correspond to the sign of the voltage difference between its tow high impedance electrical inputs. This device also has possible memory applications if bistable mode switching within the broad area laser can be achieved.

14. SUBJECT TERMS
Lasers, Smart pixels, Optical computing, Optical interconnects

15. NUMBER OF PAGES
24

16. PRICE CODE

17. SECURITY CLASSIFICATION OF REPORT	18. SECURITY CLASSIFICATION OF THIS PAGE	19. SECURITY CLASSIFICATION OF ABSTRACT	20. LIMITATION OF ABSTRACT
UNCLASSIFIED	UNCLASSIFIED	UNCLASSIFIED	UL

NSN 7540-01-280-5500
Standard Form 298 (Rev 2-89)
Prescribed by ANSI Std 239-18
298-102

TABLE OF CONTENTS

Accesion For

NTIS CRA&I ☒
DTIC TAB ☐
Unannounced ☐
Justification .....

By .....
Distribution /

Availability Codes

Dist	Avail and / or Special
A-1	

ACKNOWLEDGMENTS

The authors wish to acknowledge the staff at the National Nanofabrication Facility, along with other members of C. L. Tang's research group at Cornell University. At the USAF Photonics Center, Rome Laboratory, acknowledgment is also given to members of R. J. Michalak's group.

The authors contributed as follows. P. D. Swanson authored this report. M. A. Parker, P. D. Swanson and S. I. Libby designed and tested the devices. P. D. Swanson, J. S. Kimmet and M. A. Parker fabricated the devices.

I. INTRODUCTION

Optical processing of photonic digital signals requires a logic family with all optical inputs and outputs. This logic family should be cascadable and should switch states non-linearly with the change of input signal intensities. In order to have these attributes the gates require an all optical switching mechanism and signal gain. Signal gain can be achieved by either optically amplifying input signals or by having an output laser whose output intensity is larger than the input signals. The latter is considered the more desirable of the two, since optical signal amplification adds noise. Q-switched semiconductor lasers provide the ideal output for such gates due to their high on-off ratios and abrupt switching characteristics.[1] Previous efforts have developed NOR gates using high intensity input beams to quench the gain section within the laser cavity, thus Q-switching it off.[2] Unfortunately, such devices cannot by themselves be cascaded since their input intensity must be larger than their lasing intra-cavity light intensity; thus their output intensity will always be smaller than the required input switch intensity. OR gates that use input beams to saturate an intra-cavity absorption section suffer from the same flaw.[3] However, the same absorption section can turn off and on the laser with much lower switching powers by simply varying its applied voltage.[4,5] Figure 1 shows the relative transmission of light traveling through such an absorption section, (in this case consisting of a single quantum well laser heterostructure), for various applied voltages, while Figure 2 shows the resulting photo-current as a function of applied voltage and wavelength.

It is important to note from Figure 2 that the modulator photo-current falls drastically when the modulator bias voltage becomes positive. If the modulator was reverse biased with a current source, any photo-current less than the sourced current

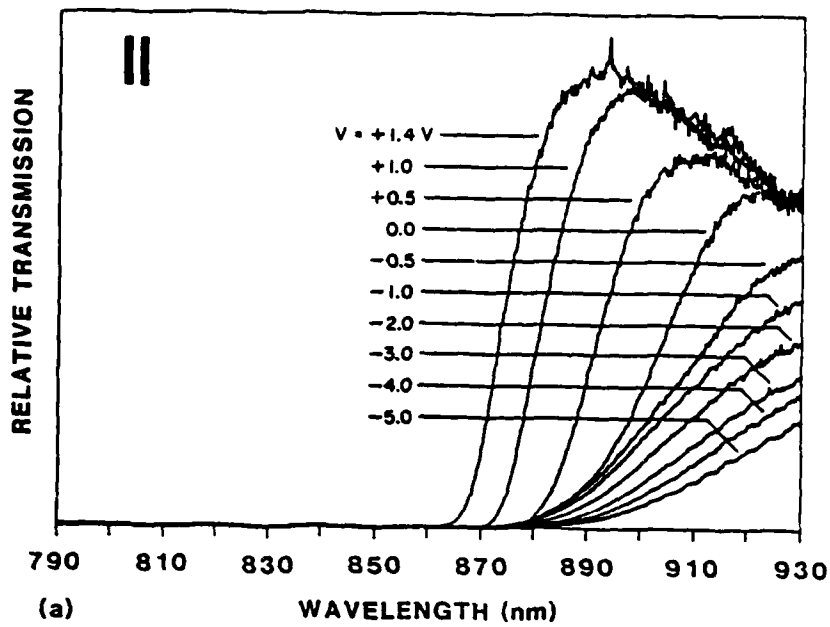

Figure 1. Relative transmission as a function of wavelength for various applied voltages.[3]

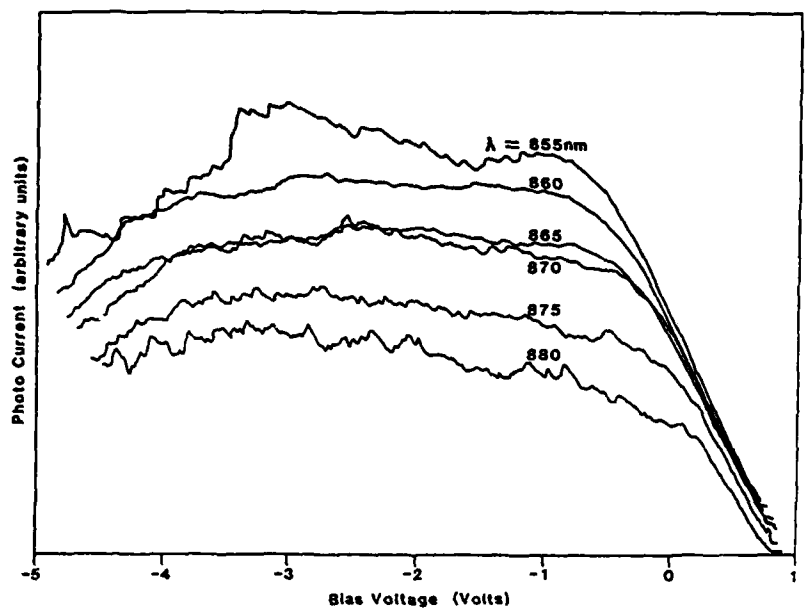

Figure 2. Photo current as a function of bias voltage for a range of wavelengths.[3]

would cause the modulator voltage to swing negative, until the combined new photo-current and leakage current matched the sourced current. Photo-currents larger than the sourced current would cause the modulator voltage to swing positive, until again the combined photo-current and leakage current equaled the sourced current. These photo-currents could be due to either intra-cavity absorption in the modulator or to absorption of an input beam by a photo detector wired in parallel to the modulator. If more than one input beam is aimed at the detector, OR functionality is achieved (see Figure 3). If the sourced current is provided by photo detectors, (Figure 4), then NOR functionality is achieved. This report details the testing of these designs with discrete Q-switched lasers and Si P-I-N detectors, while mapping the circuit design modifications made to reduce the required switching power.

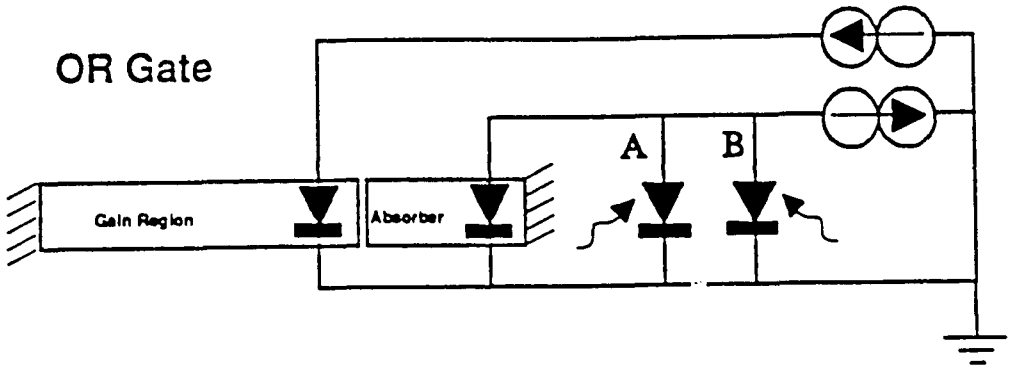

Figure 3. Schematic diagram of an all optical OR gate.

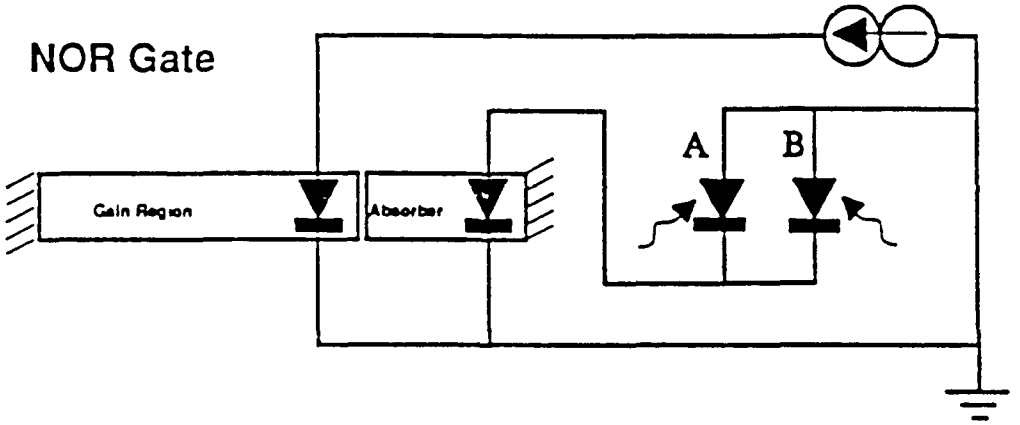

Figure 4. Schematic diagram of an all optical NOR gate.

II. ANALYSIS

In order to optimize the performance of the gates we would like to maximize both the on/off ratio of the output and the ratio between output power and minimum switching power. At the same time it would be desirable to keep the device power consumption as low as possible. The variable parameters include the laser width, the gain section length, the modulator length, the mirror reflectivity, as well as the design of the detector-modulator circuit. The switching power is simply the number of electrons required to offset the off-state photo current of the modulator multiplied by the photon energy of the input beam:

$$P_{SWITCH} = \frac{h\,c\,I_{PHOTO(off)}}{q\,\lambda} \qquad [1.]$$

In both the OR and NOR gate designs, this amount of energy is the minimum required to cause the voltage on the modulator to reverse bias. For a modulator situated right before a mirror with reflectivity constant R_1, the off-state photo current due to absorption of the spontaneous emission coming from the gain section is approximately

$$I_{PHOTO} \approx \int q\,(\,e^{\gamma_0(\nu)\,L_G} - 1\,)\,(\,1 - (\,1 - R_1\,)e^{-\alpha_{off}(\nu)\,L_M} \cdot R_1\; e^{-2\alpha_{off}(\nu)\,L_M}\,)\,d\nu\,, \qquad [2.]$$

were L_M is the length of the modulator and L_G is the length of the gain section.[6] Both $\alpha_{off}(\nu)$, the off state absorption coefficient of the modulator, and $\gamma_0(\nu)$, the gain coefficient of the gain section vary as a function of the optical frequency ν, and therefore the photo current must be integrated over the entire spontaneous emission spectrum. From

equations 1 and 2 it is evident that minimizing the switching power requires using the smallest possible modulator length.

The output power of this laser in the off state is also due to the spontaneous emission of the gain section:

$$P_{OUTPUT\Downarrow} \approx \left(hc/\lambda\right) \int \left(e^{\gamma_0(v) L_G} - 1 \right) \left(1 - R_1 \right) e^{-\alpha_{off}(v) L_M} \, dv \,, \qquad [3.]$$

The output power in the on state is a function of the gain and loss mechanisms within the laser:

$$P_{OUTPUT\Uparrow} = P_{SAT} T_1 \frac{\gamma_0 \, 2L_G - \alpha_{prop} 2L_G - \alpha_{on} 2L_M - T_1 - T_2}{2 \left[\alpha_{prop} 2L_G + \alpha_{on} 2L_M + T_1 + T_2 \right]} \qquad [4.]$$

where P_{SAT} is the saturation intensity of the gain; γ_0 is the unsaturated gain coefficient; α_{prop} is the loss coefficient due to internal losses within the gain region; α_{on} is the loss coefficient within the modulator; and $T_1=1-R_1$ and $T_2=1-R_2$ are the mirror transmission coefficients of the two output mirrors.[6] Note that the maximum functional output power occurs when

$$\gamma_0 \, 2L_G = \alpha_{prop} \, 2L_G + \alpha_{off} \, 2L_M + T_1 + T_2 \qquad [5.]$$

in order for the laser to switch off when the modulator absorption coefficient shifts from α_{on} to α_{off}. Therefore the maximum output power can be expressed as:

$$P_{OUTPUT\,(max)} = P_{SAT} \left(T_1\right) \frac{2L_M \left(\alpha_{off} - \alpha_{on} \right)}{\alpha_{prop} \, 2L_G + \alpha_{on} \, 2L_M + T_1 + T_2} \qquad [6.]$$

Equations 2 and 3 show that the off-state modulator photo current and the off-state output power increase exponentially with the gain coefficient $\gamma_{s(v)}$. Equation 4 shows that the on state output power increases linearly with $\gamma_{s(v)}$ However, Equation 6 reveals that it is $\alpha_{off} - \alpha_{on}$ which is the major factor determining the on/off ratio. α_{off} and α_{on} are determined by the voltage swing across the modulator, which is a function of both the quantum well design and the detector-modulator driving circuit.

III. LASER FABRICATION

Two section Q-switch lasers were fabricated from a standard multiple quantum well laser heterostructure, shown in Figure 5. The heterostructure consists of quantum wells centered in a p-i-n diode superimposed on a planar optical waveguide (high-index core surrounded by a low-index cladding).

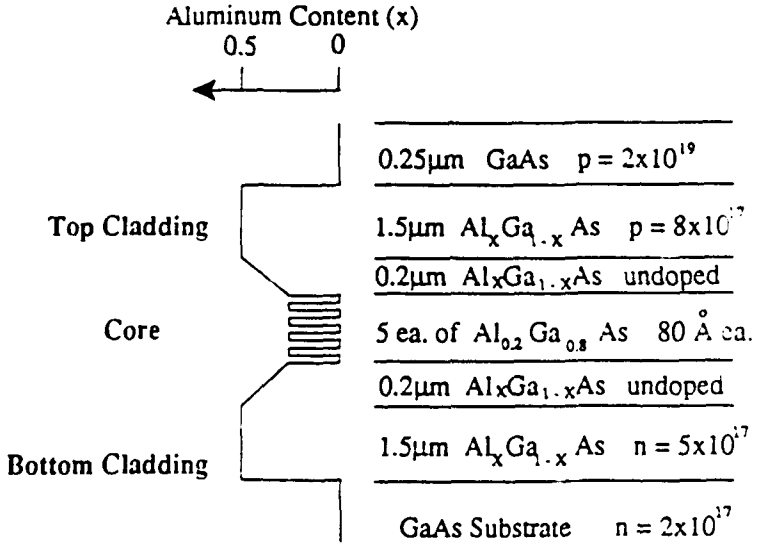

Figure 5. A standard epitaxially-grown laser heterostructure, utilizing multiple quantum wells in an active region centered within a graded-index waveguide.

The lasers require etched regions of two different depths: a deep etch that extends well into the lower cladding region for the laser mirrors, and a shallow etch to delineate the waveguides. In order to create an effective lateral index difference, the shallow etch should be within 100 nm of the top of the planar waveguide core.[7] Mirror-quality vertical walls were etched using chemically assisted ion beam etching (CAIBE).[8] Chrome, silicon dioxide or photo-resist all can be used as CAIBE etch masking materials; however, of the three, only chrome stands up well enough to produce good quality laser mirrors. For this reason chrome was used in a self-aligning process to delineate the waveguides and mirrors, while silicon dioxide and/or photo-resist was used to mask the shallow etch regions during the first stage of the deep etch. The chrome doubled as the top metal for the p-type ohmic contact, so it did not require removal after processing.

The devices were etched twice in the CAIBE. In the first etch only the regions to be deep etched were not masked. The depth of this etch was that of the difference of the two desired etch depths. After the silicon dioxide (or photo-resist) mask was removed, leaving only the chrome mask, a second etch was performed. The depth of the second etch was that of the desired shallow etch.

After the two CAIBE etches, oxygen was implanted at 60 KeV, 120 KeV, and 180 KeV at a dose of 10^{12} /cm^2 for electrical isolation between laser sections. The p-contact metallization (20 nm of titanium, 20 nm of platinum, 300 nm of gold and 170 nm of chrome) was used to mask the oxygen implant. Finally, the wafers were lapped down to 250 μM thick, and the backs were metallized with 10 nm of nickel, 40 nm of germanium, 80 nm of gold, 100 nm of silver and 70 nm of gold for the n-type ohmic contact. The contacts were alloyed at 360°C for one minute. The wafers were then cleaved, mounted and tested.

IV. DEVICE TESTING

The devices were tested using a fiber optic / electronic probe station at the Photonics Laboratory at Griffiss Air Force Base. A pulse generator, used as a clock for the gates, pulsed the gain sections of the lasers while discrete PIN detectors were connected as shown in Figures 3 and 4 to implement the OR and NOR gate, respectively. A low-power helium-neon laser was used as optical input beams. Because photo-current, not photons, Q-switch the laser, the input wavelength is only limited by the sensitivity of the detectors used.

Q-Switched Laser

Two sizes of Q-switched lasers were used to test the gates. The first consisted of a 200 μM by 20 μM gain section and a 20 μM by 20 μM modulator, separated by a 2 μM shallow etched (and oxygen implanted) gap. The second consisted of a 200 μM by 4 μM gain region and a 4 μM by 4 μM modulator, again separated by a 2 μM etched gap. Before the oxygen implant, the isolation trench between the gain section and the modulator provided resistances varying between 300 and 1000 ohms. After the implant, the pad-to-pad resistance of the 20 μM wide devices was ~1.7 Meg ohms, while the 4 μM wide pad-to-pad resistance was even higher. This resistance was crucial for the performance of the gates, since the currents determining the bias on the modulator were orders of magnitude smaller than the pump currents driving the gain section.

Figure 6 shows the threshold current of a 20 μM wide laser as a function of its modulator voltage. In operation the laser gain section should be biased just below the threshold current of the laser for a modulator voltage set at the minimum of the voltage swing provided by the detector driving circuit. The voltage swing should be large enough to insure that this current level is above threshold for the maximum modulator voltage. From Figure 1 and Equation 6, it is obvious that the larger voltage swings yield

larger maximum output intensities. However, increasing the voltage swing also increases the switching power.

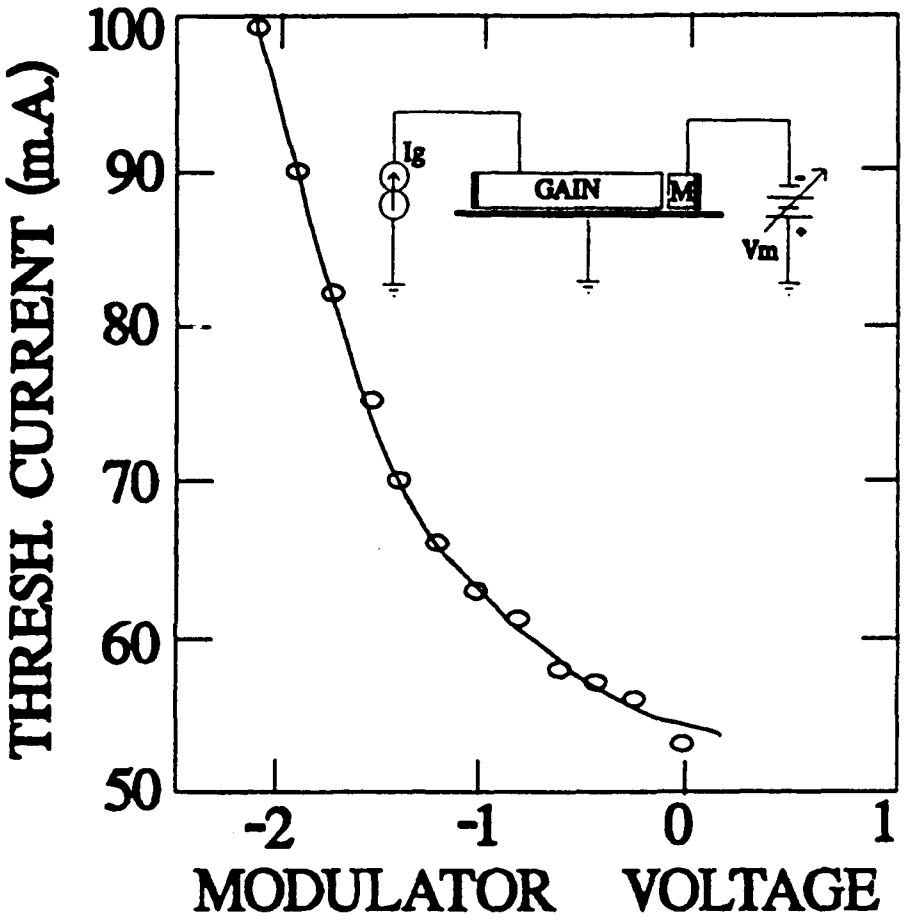

Figure 6. Threshold current of Q-switched laser as a function of the intra-cavity modulator voltage.

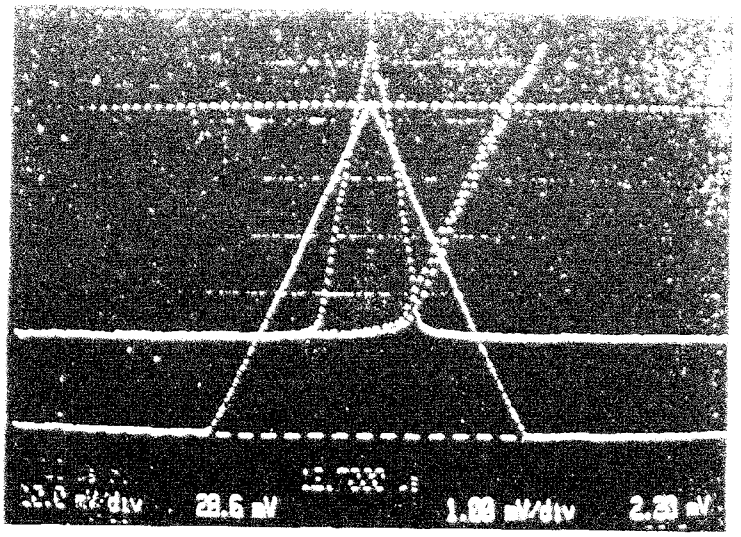

(b)

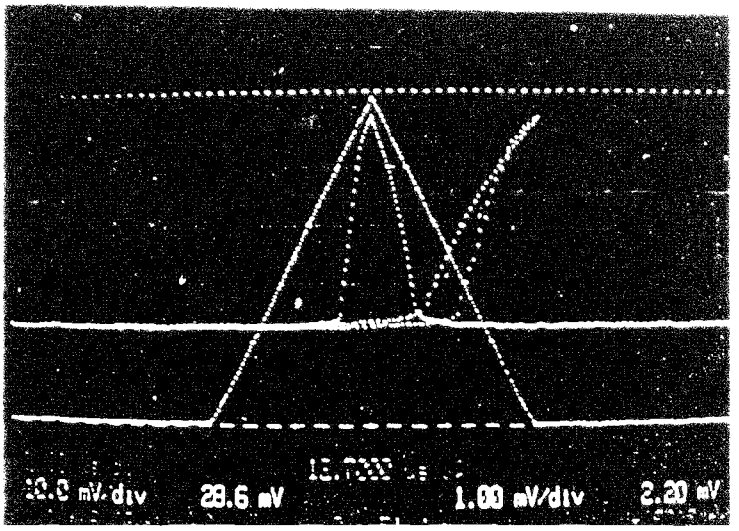

Figure 7. Output Intensity of a Q-switched laser as a function of the current biasing the gain section for a modulator current set at (a) 0 mA (b) -0.4 mA. Output Intensity and driving current are also shown as a function of time.

Figure 7 shows I-L curves for a 20 μM wide laser whose modulator is biased at two constant currents (0 mA and -0.4 mA). In both cases a modulator voltage swing is created by the difference in modulator photo current in the on and off states. For the latter case the voltage swing is large enough to produce bistability. This effect can be useful for developing single laser flip-flops or for improving the switching characteristics of logic gates.

OR Gate

The OR function was demonstrated by directing the helium-neon laser onto two PIN detectors, which were connected to a Q-switched laser as shown in Figure 3. Both 20 μM wide and 4 μM wide Q-switched lasers successfully performed the OR function, with the multi mode (20 μM) lasers yielding a higher on-off ratio and the single mode (4 μM) lasers yielding higher gain. For each case, the current source was set to the photo current of the modulator section when its bias voltage was approximately -4 volts. This current was 0.7 mA for the 20 μM square modulator, and 0.002 mA for the 4 μM square modulator. For the latter case, an input power of 3.95 mW switched on the gate, producing 83 mW of output power, and thus providing a power gain of 21. The 20 μM wide Q-switched lasers provided a gain above unity.

Figure 8 shows the emission spectrum for an OR gate using a 20 μM wide Q-switched laser. Both the logic 1 output state and the logic 0 output state are shown. The on/off ratio between these two output states is approximately 1000:1. The 4 μM wide lasers yielded similar results with an on/off ratio of better than 10:1.

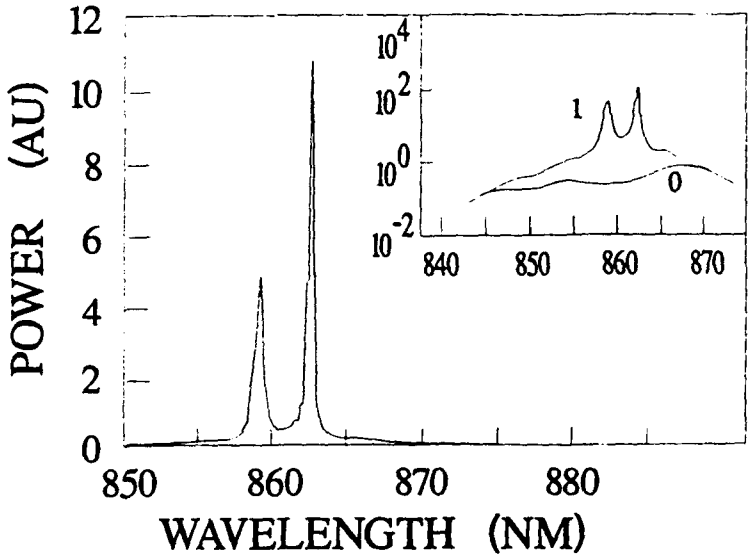

Figure 8. The emission spectrum of an OR gate using a 20 μM wide Q-switched laser for both the logic 0 and 1 output states.

NOR Gate

The NOR function was successfully demonstrated by connecting the Q-switched laser and PIN detectors as shown in Figure 4. The negative voltage bias on the detectors was set at -3 volts. As anticipated, increasing the sourced current to the modulator increased the output and switching power; however, the switching power increased at a much faster rate than the output power. For this reason, a zero mA source current yielded the best gain. Figure 9 shows the emission spectrum of a NOR gate using a 20 μM wide Q-switched laser. Both the output logic 1 and logic 0 states are shown for the current source set to zero mA. Note that at these bias levels the on/off ratio is only 3.4:1.

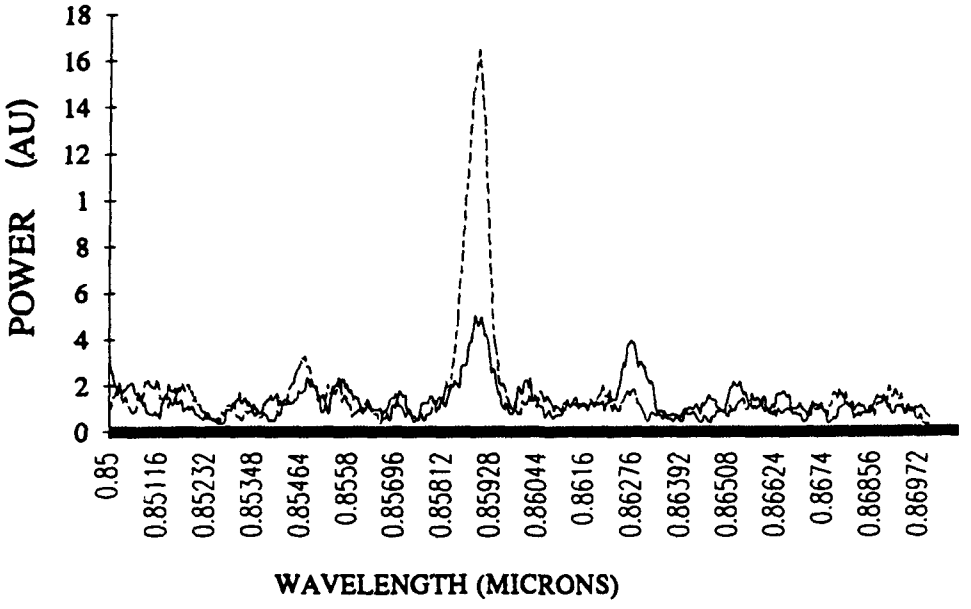

Figure 9. The emission spectrum of a NOR gate using a 20 μM wide Q-switched laser for both the logic 0 and logic 1 output states.

IV. DISCUSSION

Improvements to the driving circuits may be able to reduce the required detector photo current to achieve the same voltage swing. Figures 10a and 10b show such design improvements for the OR gate and the NOR gate respectively. In order to increase the resulting voltage swing without the use of transistors, a voltage source replaces the grounded end of the detector for each circuit. This design change requires semi-insulating substrates in order to monolithically integrate gates since the diodes no longer share a common ground.

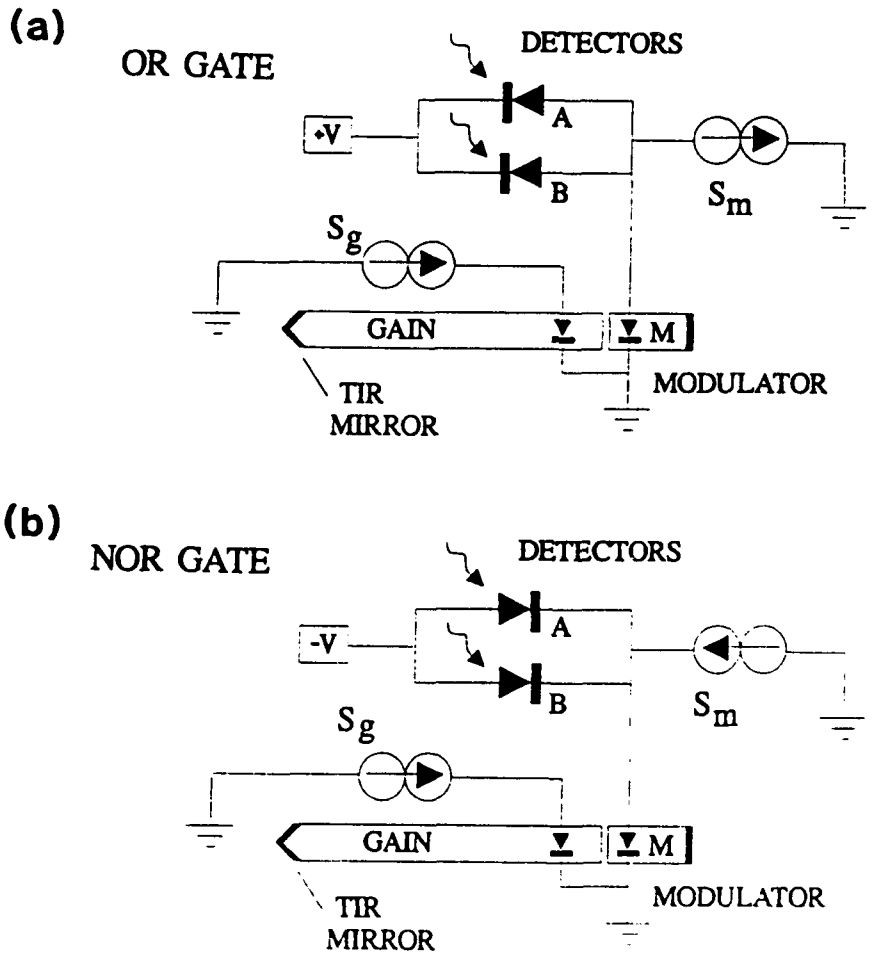

Figure 10. Schematic diagram of improved (a) OR gate and (b) NOR gate.

V. CONCLUSION

Both the OR gate design and the NOR gate design were validated, using discrete detectors and various-sized Q-switched lasers. Only gates using single mode lasers with very small area modulators demonstrated gains capable of allowing the devices to be cascaded to the input of a similar gate. Changes in the detector driving circuit should further improve switching efficiency and thus increase fan out.

VI. REFERENCES

1. C. Harder, K.Y. Lau, A. Yariv, "Bistability and Pulsations in Semiconductor Lasers with Inhomogeneous Current Injection", IEEE J. Quant. Electr. QE-18, p.1351, 1982

2. W.J. Grande, C.L. Tang, "Semiconductor laser logic gate suitable for monolithic integration", Appl. Phys. Lett., Vol. 51, p.1780, Nov. 1987

3. P.D. Swanson, M.A. Parker, S.I. Libby, "Evaluation of Laser Diode Based Optical Switches for Optical Processors", Rome Laboratory Final Technical Report RL-TR-93-145, July 1993

4. P.D. Swanson, "Characteristics of Semiconductor Optical Waveguides Fabricated by Impurity Induced Layer Disordering", Ph.D. thesis, University of Illinois, Urbana-Champaign, 1989

5. C.M. Herzinger, P.D. Swanson, K.T. Tang, T.M. Cockerill, L.M. Miller, M.E. Givens, T.A. DeTemple, J.J. Coleman, and J.P. Leburton, "Electroabsorption properties of a single GaAs quantum well", Phys. Rev. B, Vol. 44, p.13478, Dec. 1991

6. J.T. Verdeyen, Laser Electronics, Prentice-Hall, Inc., New Jersey, p.179-183, p.195-201, © 1981

7. C.F. Lin, "A New Technique for Monitoring Etched Depth in the Fabrication of Ridge-Waveguide Lasers", M.S. Thesis, Cornell University, May 1989.

8. W.J. Grande, J.E. Johnson, and C.L. Tang, "Characterization of etch rate and anisotropy in the temperature-controlled chemically assisted ion beam etching of GaAs", J. Vac. Sci. Technol. B, Vol. 8, p. 1075, Sept/Oct 1990

*U.S. GOVERNMENT PRINTING OFFICE: 1994-510-117-50012

MISSION

OF

ROME LABORATORY

Mission. The mission of Rome Laboratory is to advance the science and technologies of command, control, communications and intelligence and to transition them into systems to meet customer needs. To achieve this, Rome Lab:

a. Conducts vigorous research, development and test programs in all applicable technologies;

b. Transitions technology to current and future systems to improve operational capability, readiness, and supportability;

c. Provides a full range of technical support to Air Force Materiel Command product centers and other Air Force organizations;

d. Promotes transfer of technology to the private sector;

e. Maintains leading edge technological expertise in the areas of surveillance, communications, command and control, intelligence, reliability science, electro-magnetic technology, photonics, signal processing, and computational science.

The thrust areas of technical competence include: Surveillance, Communications, Command and Control, Intelligence, Signal Processing, Computer Science and Technology, Electromagnetic Technology, Photonics and Reliability Sciences.